

# Modélisation de la Vitesse de Propagation de Flamme Dans Une Chambre de Combustion Sphérique à Volume Constant

PROJET DE FIN D'ÉTUDES

**Maria Savall Mañó**  
**Tuteurs:** Taissir Kasraoui, Remi Bertossi  
Institut Polytechnique des Sciences Avancées  
Année 2015–2016

# Índice

ABBREVIATIONS	2
ABSTRACT	3
1. INTRODUCTION	4
2. SPHERICAL VESSEL METHOD	5
3. BURNING VELOCITY MEASUREMENT USING SPHERICAL VESSEL METHOD FOR FLAMMABLE COMPOUNDS	8
4. BURNING VELOCITY MEASUREMENT FOR FLUORINATED COMPOUNDS USING THE SPHERICAL VESSEL METHOD	13
5. CONCLUSION	16
6. BIBLIOGRAPHY	17
A. Measurements of The Laminar Burning Velocity For Mixtures of Methanol and Air From A constant-Volume Vessel Using A Multizone Model	18
B. Mathematical Solutions for Explosions in Spherical Vessels	21
C. Equations for the Determination of Burning Velocity In A Spherical Constant Volume Vessel	26
D. Burning Velocity Measurement of Fluorinated Compounds By The Spherical-Vessel Method	30
E. Impact of Dissociation and End Pressure on Determination of Laminar Burning Velocities In Constant Volume Combustion	32

## ABBREVIATIONS

- $S_u$ : Laminar burning velocity
- $x(p)$ : Burnt mass fraction at constant pressure
- $C_p$ : Specific heat
- $e$ : Specific internal energy
- $h$ : Specific enthalpy
- $m$ : Mass
- $p$ : Pressure
- $S$ : Entropy
- $T$ : Temperature
- $v$ : Specific volume
- $r_b$ : Radius of the burnt gas
- $R$ : Radius of the spherical vessel

## ABSTRACT

In this thesis, multiple burned gas zone model has been used to determine temperature distributions and its relationship between pressure distribution and mass fraction in a constant-volume vessel. The constant-volume spherical vessel has been used for determining distributions of elevated initial temperatures and pressures. Multizone model allows us to find the laminar burning velocity and the intervals of temperature, pressure and equivalence ratios it can be found.

Laminar burning velocity has been found with different methods to compare with multizone model theoretically and experimentally. Various of equations were compared for their accuracy.

# 1. INTRODUCTION

The burning velocity is the characteristic propagation rate of laminar premixed flames, in other words the burning velocity  $S_u$  is defined as the velocity at which unburned gases move through the combustion wave in the direction normal to the wave surface. They play essential roles in determining the ignition delay, the thickness of the wall quench layers, the minimum ignition energy. Moreover, a detailed knowledge of laminar pre-mixed flames will provide knowledge to heat release rates, flammability limits, propagation rates, quenching, and emission characteristics. The laminar burning velocity is a function of both fuel/oxidant ratio and temperature and pressure of the system. There are several ways to determine the laminar burning velocity. The most convenient one is the constant-volume bomb method which uses a spherical vessel with central ignition. The aim of using a spherical vessel with central ignition is to generate laminar burning velocities for varying conditions. Fortunately, using a spherical vessel with central ignition with a multizone model provides this to us with a single test.

The fuel is burnt in turbulent combustion mostly. In order to ease the analysis, a set of assumptions is made. These can be classified as uniform pressure, negligible heat loss or gain, no buoyancy, isentropic compression of the unburnt gas, spherical flame front and ideal gas behavior.

The spherical method is widely used for the flammable gases, because it provides experimental accuracy as well as operational simplicity: the burning velocity of a compound together with its temperature and pressure dependence is obtained simultaneously. On the other hand, there is a concern about using spherical vessel method for weakly flammable compounds. For a compound with low burning velocity such as  $\text{NH}_3$  the buoyancy force may distort the flame front which cannot be regarded as spherical. In other words, it is impossible to use our assumption that the flame front is spherical and smooth.

## 2. SPHERICAL VESSEL METHOD

The assumptions and mathematical derivations for the pressure and burned and unburned gas temperatures are presented for the single burned gas zone model. The single burned gas zone model was extended to two burned zone and then to multiple zones. The reason of dividing the spherical vessel into multiple zones is the two zone analytical model neglects the burnt temperature gradient. This simplification was shown not to affect the  $x(p)$  results within a perfect gas. However, when a both burnt temperature gradient and dissociation are allowed, this may no longer hold true: enhanced dissociation near the core of the vessel may affect the mass averaged burnt temperature, leading to different results for  $x(p)$  as well.

In a two zone model, both the burnt and unburnt zones have uniform temperatures and compositions:

$$v_t = x \cdot v_b + (1 + x) \cdot v_u \quad (1)$$

$$e_t = x \cdot e_b + (1 + x) \cdot e_u \quad (2)$$

Having a conversation of specific volume and specific internal energy:

$$x = \frac{p - p_i \cdot (p)}{p_e - p_i \cdot f(p)} \quad (3)$$

Knowing that  $f(p)$  in equation(3) is:

$$f(p) = \frac{\gamma_b - 1}{\gamma_u - 1} + \left( \frac{\gamma_u - \gamma_b}{\gamma_u - 1} \right) \cdot \left( \frac{P}{P_i} \right)^{\frac{\gamma_u - 1}{\gamma_u}} \quad (4)$$

In the multi zone model, flame prorogation is seen as the consecutive consumption of unburned mixture within the zones. Before ignition, the mass in the spherical vessel divided into  $n$  zones. At the time, when combustion has just began in the bomb, the flame front will consume zone 1 first. As a result, the temperature and hence the pressure of zone 1 will increase by the ideal gas assumption, thereby compressing the rest of the unburned gas and increasing pressure inside the vessel to a higher value. After the consumption of the first zone, consumption of the second zones will take place at a higher pressure than the initial pressure. When the flame front is passing through the  $n$ th zone, the combustion of this zone takes place at a temperature of  $T_{u,n-1} (> T_i)$  and a constant pressure  $P_{u,n-1}(P_i)$ . After the flame has consumed the  $n$ th zone, it is assumed to be adiabatic. Previous work has shown that when the burning velocities are above  $20 \frac{cm}{s}$ , the effect of buoyancy is less than 0.5% on the observed burning velocity. Subsequent combustion further compresses the burned gas and the unburned gas. As a result, temperature and density gradients are established in the burned gas region.

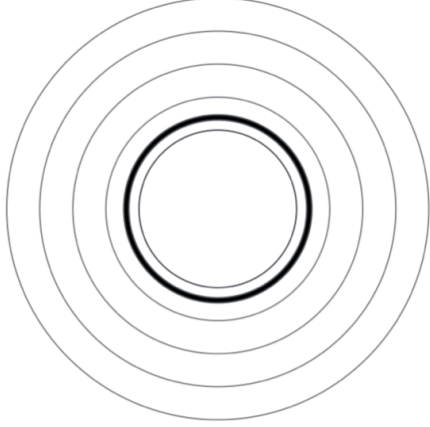


Figure 1: Zone 2 burning

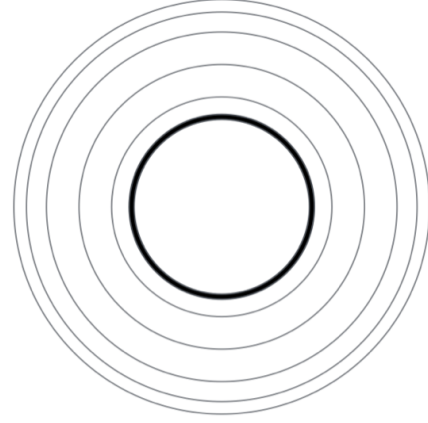


Figure 2: Zone 1 burning

The approach for two zones can be extended to multiple zone model. Neglecting heat loss to the vessel wall:

$$v_t = \sum_{j=1}^{n=1} x_j \cdot v_{bj} + x_n v_{bn} + \left[ 1 - \sum_{j=1}^1 x_j \right] \cdot v_u \quad (5)$$

$$e_t = \sum_{j=1}^{n=1} x_j \cdot e_{bj} + x_n e_{bn} + \left[ 1 - \sum_{j=1}^1 x_j \right] \cdot e_u \quad (6)$$

$$x = \sum_{n=1}^N x_n \quad (7)$$

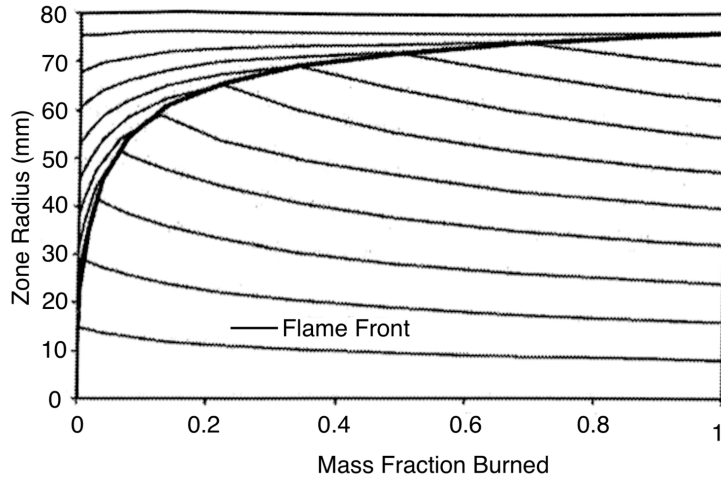


Figure 3: Mass fraction in function of the zone radius

In Figure 3 we are able to see how the radius of each zone varies during the propagation of the flame front. As the flame front travels through the combustion bomb, each zone burns and an increase in the radius of that zone takes place. This is due to the expansion of the products of combustion immediately behind the flame front. When the flame front has passed the zone, recompression of the zones takes

place due to the expansion of the next zone. Due to the recompression, a decrease in the radius and hence the volume of the burned zones takes place. This results in an increase in the temperature of the burned gas zones, which establishes the radial burned gas temperature gradient. As the first burned zone is hotter than the outer zones it can be seen that the zone 1 finishes with a larger radius.

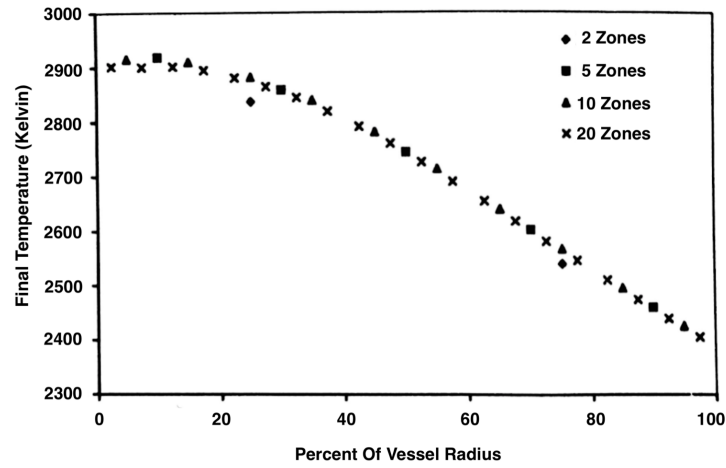


Figure 3: Final variation of temperature with the zones in the equal radius model with initial conditions of 1 bar and 298.1 K for stoichiometric methane-air mixture



### 3. BURNING VELOCITY MEASUREMENT USING SPHERICAL VESSEL METHOD FOR FLAMMABLE COMPOUNDS

The burning velocity calculations are based on using a spherical closed vessel filled with homogeneous combustible mixture. At time  $t = 0$ , the mixture is ignited at the center; a spheric flame front is established and begins to propagate outwardly to reach the wall. The following assumptions are used:

- The unburned gas is initially at rest and the gas has a uniform temperature and composition.
- The thickness of the reaction zone is negligible, and the flame front is smooth and spherical.
- The burnt gas fraction  $x$  is at local thermodynamic and chemical equilibrium.
- The unburned gas fraction  $(1 - x)$  is at local equilibrium but with fixed chemical composition.
- The pressure within the combustion vessel is a function of the time and independent of the flame front.
- The compression for the whole gas is adiabatic and reversible.
- The gas behaves as a semi perfect gas.
- The effects of body forces and of radiative energy transfer can be neglected.
- There is no heat transfer between burned and unburned gas.

From the equation of continuity:

$$\frac{dm_u}{dt} = -A\rho_u S_u \quad (8)$$

Combustion in a constant volume spherical vessel, the mass of unburnt gas at any instant:

$$m_u = \frac{4}{3}\pi[(R^3 - r_b^3)] \quad (9)$$

From the equations (8) and (9) we arrive to:

$$\frac{dm_u}{dt} = \frac{4}{3}\pi \left[ (R^3 - r_b^3) \frac{d\rho_u}{dt} - 3 \cdot r_b^2 \rho_u \frac{dr_b}{dt} \right] = -A\rho_u S_u \quad (10)$$

From equations (8) and (10) and knowing that  $A = 4\pi \cdot r_b$ :

$$S_u = \frac{dr_b}{dt} = \frac{R^3 - R_o^3}{3r_b^2 \rho_u} \cdot \frac{d\rho_u}{dt} = S_s - S_g \quad (11)$$

Considering that the compression is adiabatic,  $P = Cp^\gamma$ :

$$S_u = \frac{dr_b}{dt} = \frac{R^3 - R_B^3}{3R_b^2 \gamma_u \cdot P} \frac{dP}{dt} \quad (12)$$

The equation (12) is called: **The unburnt gas equation for the burning velocity of Fiock & Marvin.**

Alternative forms of these equations can be obtained by considering the burnt gas behind the flame front. Combustion in a constant volume vessel:

$$m_u = m_o - m_b \quad (13)$$

$$\frac{dm_u}{dt} = -\frac{dm_b}{dt} \quad (14)$$

From equation (8) and (14), we obtain:

$$S_b = \frac{1}{A\rho_u} \cdot \frac{dm_b}{d} \quad (15)$$

Being  $S_b$  a property of the burnt gas.

For a spherical flame front:

$$m_b = \frac{4}{3}\pi r_b^3 \bar{\rho}_b \quad (16)$$

The mean density allows us to obtain non-uniform properties of the gas behind the flame front due to recompression:

$$\bar{\rho}_b = \frac{3}{r_b^3} \int_0^{r_b} \rho_b \cdot r^2 dr \quad (17)$$

From the equations (16) and (17) we get:

$$\frac{dm_b}{dt} = \frac{4}{3}\pi \left[ r_b^3 \frac{d\bar{\rho}_b}{dt} + 3 \cdot r_b^2 \cdot \bar{\rho}_b \frac{dr_b}{dt} \right] \quad (18)$$

From equations (15) and (18):

$$S_b = \frac{\bar{\rho}_b}{\rho_u} \frac{dr_b}{dt} + \frac{r_b}{3\rho_u} \frac{d\bar{\rho}_b}{dt} \quad (19)$$

Considering adiabatic compression  $P = C' \bar{\rho}_b^{\gamma_b}$  we arrive to:

$$\frac{d\bar{\rho}_b}{dt} = \frac{\bar{\rho}_b}{\gamma_b P} \frac{dP}{dt} \quad (20)$$

$$S_b = \frac{\bar{\rho}_b}{\rho_u} \left[ \frac{dr_b}{dt} + \frac{r_b}{3\gamma_b P} \frac{dP}{dt} \right] \quad (21)$$

### The burnt equations for the burning velocity

Substituting we obtain:

$$r_b = R \cdot \left[ \frac{\frac{\rho_u}{\rho_o} - 1}{\frac{\rho_u}{\rho_o} - \alpha} \right]^{\frac{1}{3}} \quad (22)$$

The calculated values of  $r_b$  are nearly always less than the observed radius. This difference suggests the existence of a reaction zone of significant thickness, particularly during the early stages when the spatial velocity is high. Values based on the low range pressure record are constantly nearer the observed radius than values from the high range record. The discrepancy between the calculated and observed flame radius suggests a lack of equilibrium in the burnt gas, probably confined to a reaction zone adjacent to the flame front. With the equations derived, an estimate of the degree of lack of equilibrium is possible.

Consider the parameter  $\alpha$  which is defined as the ratio of the mean density of the burnt gas to the density of the unburnt mixture before ignition:

$$\alpha = \frac{\bar{\rho}_b}{\rho_o} = \frac{\bar{\rho}_b}{m_u} \frac{T_o}{\bar{T}_b} \frac{P}{P_o} \quad (23)$$

Using the observed maximum pressure,  $P_e$ ,  $m_e$  and  $T_e$ , corresponding to final conditions in the burnt gas at the flame front, may be calculated assuming equilibrium conditions. An approximate value of  $\alpha_e$  may be calculated:

$$\alpha_e = \frac{m_e}{m_o} \frac{T_o}{T_e} \frac{P_e}{P_o} \quad (24)$$

In all cases  $\alpha_e$  is less than unity. Since the total mass of gas in the vessel remains constant, the mean density of the products when the flame has reached the bomb wall must equal the initial density of the unburnt mixture:

$$\rho_b = \alpha \rho_o \quad (25)$$

Hence  $\alpha_e$  should have a value of unity at the end of the process. The discrepancy must therefore be attributed to  $P_e$  and  $\frac{m_e}{T_e}$  being too low.

- Consider  $P_e$ : an error could arise from:

- Incorrect calibration of the pressure measuring system
- Inadequate transient response of the pressure transducer

Use of the correct value would lower  $\alpha_e$  still further.

- Consider  $\frac{m_e}{T_e}$  instead of mean value of  $\frac{m_e}{T_e}$ :

- The temperature at the flame front is less than that at the centre of the vessel. Thus  $T_e$  is less than mean value of  $T_e$ .
- The difference between  $m_e$  and mean value of  $m_e$  is small compared with the difference between  $T_e$  than mean value of  $T_e$ .

Hence the use of mean temperatures to calculate  $\alpha_e$  would yield even lower values than those obtained by using flame front temperatures.

The only term left to account for the discrepancy between the deserved and expected values of:  $\alpha_e$  is the temperature of the burnt gas. It appears that the calculated equilibrium value of flame front temperature is too high. There are two factors which may account for the calculated value of  $T_b$  being too high:

- Combustion may not occur adiabatically due to heat loss. But, the quantity of heat loss by radiation up to the time the flame reaches the bomb wall is negligible. Conductive heat loss, due to buoyancy, is likely to be longer for slow burning mixtures, and should lead to lower values of  $\alpha_e$  for the rich and lean mixtures tested. Therefore, heat loss can not explain discrepancy.
- The assumption that equilibrium is attained immediately behind the flame front may not be justified: insufficient time may be available for the reactions to go to completion. If this is so then at any air/fuel ratio the thickness of such a reaction zone should increase with flame speed.

The lowest value of  $\alpha_e$  coincides with the greatest observed spatial velocity. Thus if a non-equilibrium condition exists at the end of the process ( $\alpha_e < 1$ ); on even greater departure from equilibrium probably exists over the initial stages since the spatial velocity is then higher.

Using the alternative approximate expression for  $\alpha$ :

$$\alpha = \frac{m_b T_e P}{m_e T_b P_e} \quad (26)$$

which must yield the correct value of  $\alpha_e$  (unity).

All previous burning velocity equations have been based on the assumption that chemical equilibrium exists in the burnt gas. In the burning velocity equation any such lack of equilibrium is partly allowed for by using the dimensionless density ratio  $\rho$  calculated from the above equation.

$t$ msec	$r_b$ in	$dr_b/dt$ in./sec	$P$ Low	$lb/in^2$ abs. High	$dP/dt$ Low	$lb/in^2$ msec High	$T_U$ R	$M_b$	$T_b$ R	$\alpha$
0	0.0823	—	12.09	12.09	—	—	531.9	29.01	4622	0.1248
1	0.4767	391	12.11	12.09	0.054	—	531.9	29.01	4622	0.1248
2	0.8699	395	12.27	12.15	0.328	0.215	532.6	29.01	4623	0.1255
3	1.2623	388	12.65	12.57	0.912	0.660	537.5	29.01	4626	0.1297
4	1.6437	371	14.20	13.58	1.808	1.428	548.8	28.99	4635	0.1399
5	1.9949	325	16.69	15.56	—	2.667	569.3	28.98	4650	0.1598
6	2.2948	281	—	19.17	—	4.667	602.3	28.96	4667	0.1960
7	2.5556	237	—	25.23	—	7.674	648.6	28.93	4694	0.2563
8	2.7730	202	—	35.84	—	12.121	713.0	28.89	4727	0.3611
9	2.9599	172	—	57.03	—	28.205	808.1	28.86	4761	0.5689
10	3.1080	121	—	87.50	—	24.937	907.0	28.83	4779	0.8679

Tabla 1: Abridged observations and results for stoichiometric acetylene–air mixture

In the Table (1) we have:

- Mixture composition: 7,72 per cent acetylene in dry air (by volume)
- Spark: gap 0,040 in; max. voltage=6 kV; max energy=18 mJ
- Vessel radius: 3,153 in
- Initial conditions  $P_0 = 12,09 lb/in^2$  abs;  $T_e = 71,9^\circ F$
- Molecular weight of unburnt mixture: 28.63
- Observed maximum pressure:  $P_e = 100,9 lb/in^2$  abs
- Properties of burnt gas at  $P_e$ :  $M_e = 28,82$ ;  $T_e = 4786 * R$

## 4. BURNING VELOCITY MEASUREMENT FOR FLUORINATED COMPOUNDS USING THE SPHERICAL VESSEL METHOD

The burning velocity:

$$S_u = \frac{R}{3} \left[ 1 - (1-x) \cdot \left( \frac{P_0}{P} \right)^{\frac{1}{\gamma_u}} \right]^{\frac{-2}{3}} \cdot \left( \frac{P_0}{P} \right)^{\frac{1}{\gamma_u}} \frac{dx}{dt} \quad (27)$$

In order to use this equation, we have to obtain the relationship of  $P$  with  $x$ ,  $\gamma_u$ ,  $r_f$ , and burned and unburned gas temperatures  $T_u$  and  $T_b$  by equilibrium calculation at a constant volume condition. Here  $\gamma_u$  was obtained from the averaged value at the initial gas temperature  $T_0$  and the instantaneous unburned gas temperature  $T_u$ . Then, these relationships were applied to the experimentally measured pressure  $P$ , and finally obtained  $S_u$  by solving the equation (27).

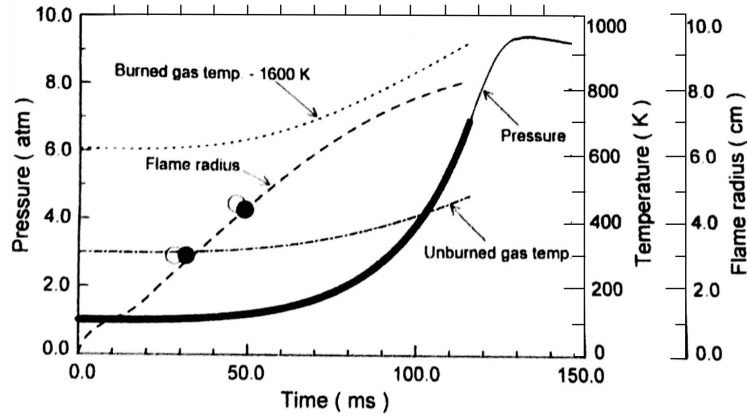


Figure 4: The experimental result for HFC143/air mixture.  $\phi = 0,94, T_0 = 300K$ , and  $P_0 = 1,0atm$ . The solid curve is the measured pressure. The broken dotted, and dotted-broken curves are calculated values of  $r_f$ ,  $T_b$  and  $T_u$ . The filled and open circles are the arrival time at ion probes in the lower and upper part of the vessel.

The consistency between the calculated  $r_f$  and the measured arrival time indicates that the spherical vessel method is valid in this case.

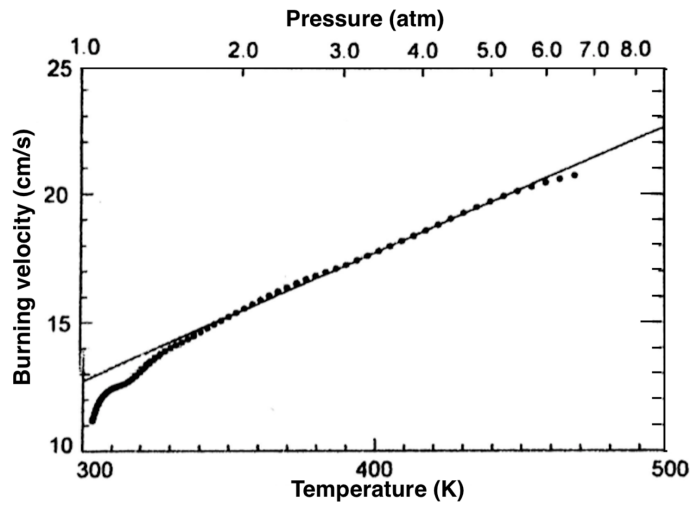


Figure 5: Burning velocity of HFC-143/air mixture.  $\phi = 0,94, T_0 = 300K$ , and  $P_0 = 1,0atm$ . The dotted curve is the experimentally obtained burning velocity. The solid curve is the result of the fitting by equation (27) in the text

Figure (5) shows temperature and pressure dependence of the burning velocity of HFC-143/air mixture.

The obtained burning velocity  $S_u$  has been fitted to:

$$S_u = S_{u0} \left( \frac{T}{T_s} \right)^\alpha \cdot \left( \frac{P}{P_s} \right)^\beta \quad (28)$$

$T_s = 298K$ ,  $P_s = 1atm$ ,  $S_{u0}$  is the burning velocity at  $T_s$  and  $P_s$  and  $\alpha$  and  $\beta$  indicate coefficients of temperature and pressure dependence.

To assess the accuracy of the spherical vessel method, the burning velocities of  $CH_4$  and  $C_3H_8$  were measured:

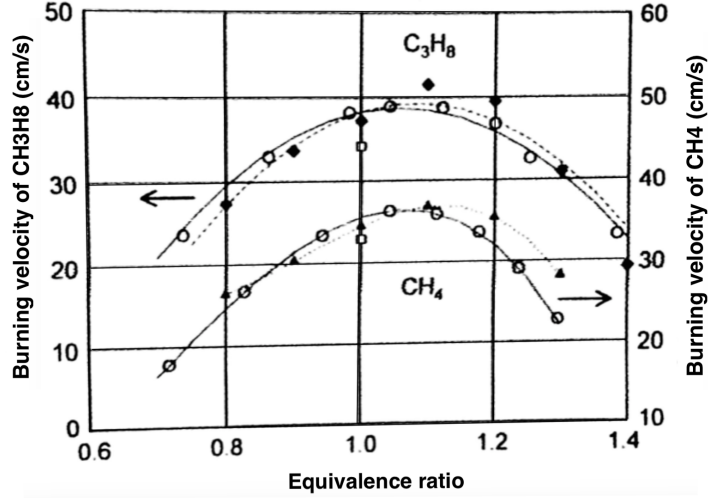


Figure 6: Burning velocity of  $CH_4$  and  $C_3H_8$  as functions of equivalence ratio. Open circle and solid curve are the present results; open square is by Hill and Hung [12]; filled diamond and broken curve are by Metghalchi and Lecl [10]; filled triangle and dotted curve are by Iijima and Takeno [11]. All the data are obtained by the SV method.

Composition	$S_{u0}$				$\alpha$		$\beta$	
	$S_{u,0,max}$	$s_1$	$s_2$	$\phi_{max}$	$\alpha_1$	$\alpha_2$	$b_1$	$b_2$
<b>HFC-32</b>	6.7	-22.3	6.99	1.08	1.97	0.47	-0.055	-0.29
<b>HFC-143</b>	13.1	-38.3	17.8	1.05	1.87	-0.47	-0.17	0.072
<b>HFC-143a</b>	7.1	-39.5	52.5	1.02	2.32	-2.00	-0.18	-0.074
<b>HFC-152a</b>	23.6	-93.9	-49.2	1.09	1.89	-0.41	-0.22	0.022
<b>CH<sub>4</sub></b>	36.5	-217	-180	1.07	1.88	-0.095	-0.36	-0.13
<b>C<sub>3</sub>H<sub>8</sub></b>	38.7	-138	5.8	1.06	1.89	-1.46	-0.27	0.54

Tabla 2: Dependence of burning velocity on temperature, pressure and  $\phi$

- $\alpha$  and  $\beta$  are coefficients for temperature and pressure dependence

Property	Method	HFC-32	HFC-143	HFC-143a	HFC-152a	CH <sub>4</sub>	C <sub>3</sub> H <sub>8</sub>	Reference
<b>Burning velocity</b> (cm s <sup>-1</sup> )	SV	6.7 <sup>a</sup>	13.1 <sup>a</sup>	7.1 <sup>a</sup>	23.6 <sup>a</sup>	36.5 <sup>a</sup>	38.7 <sup>a</sup>	This work
	SV					36.9 <sup>c</sup>		[10]
	SV					32.9 <sup>b</sup>	34.2 <sup>b</sup>	[11]
	SV					32.9 <sup>b</sup>	34.2 <sup>b</sup>	[12]
	Tube	6,7 <sup>d</sup>		6,7 <sup>d</sup>	23,0 <sup>d</sup>	37,0 <sup>d</sup>	39,0 <sup>d</sup>	[8]
	Calculation	6,7 <sup>b</sup>				40.7 <sup>b</sup>		[2]
Range <sup>e</sup> (%)	16.0-22.0	7,5-13,0	9,0-12,0	6,0-10,0				This work
<b>Flammability limits</b> LFL-UFL(%)		13.3-29.3	6.2-22.6	7.4-17.0	4.35-17.5	4.9-15.8	2.1-9.5	[4]

Tabla 3: Burning velocities and flammability limits for compound-air mixtures

- <sup>a</sup> Maximum burning velocity at 298 K and 1 atm.
- <sup>b</sup> Burning velocity at  $\phi = 1$ , 298 K and 1 atm.
- <sup>c</sup> Maximum burning velocity at 291 K and 1 atm.
- <sup>d</sup> Maximum burning velocity at 296 K and 1 atm.
- <sup>e</sup> The range of concentration where ignition was successfully done.

Direct measurement of flame propagation showed that a flame with a larger burning velocity is less affected by buoyancy than those with smaller burning velocity. For HFC-143 concentration that is far from stoichiometric, the flame shapes were distorted by buoyancy. For the concentrations that were used for the measurements, the burning velocity was obtained with good accuracy and buoyancy effects were negligible. Thus the spherical vessel method is appropriate for determining the burning velocity even for weakly flammable HFCs.



## 5. CONCLUSION

- A temperature difference exists between the first and the last burned gas zones.
- The relationship between the pressure rise and the burned mass fraction is nonlinear.
- The burned gas temperature profile has an effect on the end pressure for flammable compounds.
- The multi zone burning velocity technique has been successfully used for the determination of the laminar burning velocities of the flammable compounds.
- The spherical vessel method is appropriate for determining the burning velocity even for weakly flammable HFCs.

## 6. BIBLIOGRAPHY

- Impact of dissociation and end pressure on determination of laminar burning velocities in constant volume combustion (C.C.M. Luijiten, E. Doosje, J.A. van Oijen, L.P.H. de Goey, 2009)
- [www.elsevier.com/locate/ijts](http://www.elsevier.com/locate/ijts)
- Mathematical Solutions for Explosions in Spherical Vessels (Derek Bradley and Alan Mitcheson, 1976)
- Measurements of the laminar burning velocity for mixtures of methanol and air from a constant-volume vessel using a multizone model (Khizer Saeed, C.R. Stone, December 2003)
- Burning velocity measurement of fluorinated compounds by the spherical-vessel method (Kenji Takizawa, Akifumi Takashashi, Kabuki Tokuhashi, Shigeo Kondo, Akira Sekiya, June 2004)
- Equations for the Determination of Burning Velocity in a Spherical Constant Volume Vessel (C. J. Rallis and G. E. B. Tremeer, October 1962)
- Course of subject of Combustion of ITU (Istanbul)
- Course of subject of Combustion of UPV (Valencia)

## A.

# Measurements of The Laminar Burning Velocity For Mixtures of Methanol and Air From A constant-Volume Vessel Using A Multizone Model

## Abstract

- A multiple burned gas zone model has been used to determine the temperature distribution within the burned gas and the relationship between the pressure rise and the mass fraction burned in a constant-volume vessel.
- A constant-volume spherical vessel has been used for measuring burning notes for liquid fuels at elevated initial temperatures and pressures
- Using the multizone model the laminar burning velocity has been found for mixtures of methanol-air with initial temperatures of 293.15K and 425K, initial pressures of 0.5 bar, 1.0 bar, 2.0 bar and 3.5 bar, and equivalence ratios of 0.8 to 1.6.
- The laminar burning velocities were fitted to a seven-term equation to describe the effects of stoichiometry, pressure and temperature.

## Introduction

- Laminar premixed flames have a characteristic propagation rate, called the burning velocity. The burning velocity  $S_u$  is more precisely defined as the velocity at which unburned gases move through the combustion wave in the direction normal to the wave surface.
- Laminar burning velocities play essential roles in determining the ignition delay (affects the range of equivalence ratios over which an engine can be operated), the thickness of the wall quench layers and the minimum ignition energy
- A detailed knowledge of laminar pre-mixed flames will provide knowledge to heat release rates, flammability limits, propagation rates, quenching, and emission characteristics.
- There are two methods for determining a laminar burning velocity : stationary and nonstationary (the counterflow-burner method and the constant-volume method).
- The counterflow-burner technique is convenient for both liquid and gaseous fuels, with good control of mixture composition. it is best suited for the pressures and temperatures close to ambient.
- The constant-volume bomb method uses a spherical vessel with certain ignition and relies on measurements taken after the early stages of flame propagation, during which there is a significant pressure rise.
- The laminar burning velocity is a function of not only the fuel/oxidant ratio but also the temperature and pressure of the system and the presence of any diluents in the mixture.

## Modeling

- The single-burned-zone model was extended to two burned zones and then to multiple zones. The mass in the spherical vessel can be divided into the multiple-zones in a number of ways. The two ways used here are equal mass zones (EQM) or equal radial zones (EQR). In the multizone model, flame propagation is seen as the consecutive consumption of unburned mixture within the zones. Before ignition, the mass in the spherical vessel divided into  $n$  zones. At the time, when combustion has just begun in the bomb, the flame front will consume zone 1 first. As a result, the temperature and hence pressure of zone 1 will increase, thereby compressing the rest of the unburned gas and increasing the pressure inside the vessel to a higher value. After

the consumption of the first zone, consumption of the second zones will take place at a higher pressure than the initial pressure, When the flame front is passing through the  $n$ th zone, the combustion of this zone takes place at a temperature of  $T_{u,n-1}$  ( $> T_i$ ) and a constant pressure  $P_{u,n-1}$  ( $> P_i$ )

- After the flame has consumed the  $n$ th zone, it is assumed to be adiabatic
- Subsequent combustion further compresses the burned gas and the unburned gas. Temperature and density gradients are established in the burned gas region. In each zone will be at different temperatures, they each have a different composition. Equilibrium will be solved for  $CO, CO_2, H_2O, H_2, H, OH, O, N_2, NO, O_2$  at each temperature.
- These equilibrium calculations are solved by minimizing the Gibbs energy

## Model result

When the combustion ends in a spherical vessel, the radial temperature distributions for EQR model are shown.

To obtain accurate results and to reduce the run time of simulation, it was decided to use 10 zones and 200 steps for all the investigations.

When the flame front has passed the zone, recompression of the zones take place due to the expansion of the next zone. Due to the recompression, a decrease in the radius and hence the volume of the burned zones takes place. This results in an increase in the temperature of the burned gas zones, which establishes the radial burned gas temperature of the burned gas zones, which establishes the radial burned gas temperature gradient. As the first burned zone is hotter the outer zones, zone 1 finishes with a larger radius

The pressure variation with the mass fraction obtained in this study is nonlinear.

The maximum error in the pressure with the varying mass fraction is for stoichiometric combustion.

## Experimental Apparatus

The apparatus consists of the combustion vessel and the heating system, ignition circuit gaseous and liquid fuel handling system and data acquisition system.

The spherical test vessel is provided with central ignition electrodes and it can withstand a pressure of 34 bar.

The combustion vessel is placed inside an oven. It is fitted with a fan, a temperature controller and an air baffle plate.

Gaseous fuel air mixtures are prepared by using their partial pressures. For liquid fuel-air mixture preparation, a calibrated amount of liquid fuel is injected.

The methanol was injected through a calibrated injector, and there were then two independent checks on the air-fuel ratio (AFR). The pressure and the temperature in the vessel were measured before and after addition of the fuel.

Previous work has shown that when the burning velocities are above  $20 \frac{cm}{s}$  the effect of buoyancy is less than 0.5 % on the observed burning velocity

## Burning Velocity Calculation

The use of multizone model for the determination of the laminar burning velocity is explained below.

The burning velocity calculation are based on using spherical closed vessel filled with homogeneous combustible mixture. At time  $t=0$ , the mixture is ignited at the center; a spheric flame front is established and begins to propagate out — to reach the wall. The following assumptions are used:

- The unburned gas is initially at rest and the gas has uniform temperature and composition
- The thickness of the reaction zone is negligible, and the flame front is smooth and spherical

- The unburned gas fraction  $x$  is at local thermodynamic and chemical equilibrium
- The unburned gas fraction  $(1-x)$  is at local equilibrium but with fixed chemical composition.
- The pressure within the combustion vessel is a function of time and independent of the flame front.
- The compression for the whole gas is adiabatic and reversible.
- The gas behaves as a semiperfect gas.
- The effects of body forces and of radiative energy transfer can be neglected.
- There is no heat transfer between the burned and unburned gas.

Consider on elemental shell thickness  $dr_i$  at radius  $r_i$ . If the burned gas had not expanded, then an element  $dr_i$  would be the thickness of a shell at the temperature  $T_i$  and pressure  $P_i$ . Its volume:

$$4\pi r_i^2 dr_i$$

By expansion we have  $r_i \rightarrow r_b$ ,  $P_i \rightarrow P$ ,  $T_i \rightarrow T_u$ . Then we have its volume:

$$4\pi r_i^2 dr_i \left( \frac{T_u P_i}{T_i P} \right)$$

Since the thickness of the shell is equal to  $S_u dt$ , its volume:

$$4\pi r_b^2 S_u dt$$

Being  $S_u$  the burning velocity. However, the unburned gas is assumed to be undergoing isentropic compression;

$$T_u = T_i \left( \frac{P}{P_i} \right)^{\frac{\gamma_u - 1}{\gamma_u}} \quad (29)$$

We obtain for the burning velocity:

$$S_u = \left( \frac{dr_i}{dt} \right) \left( \frac{r_i}{r_b} \right)^2 \left( \frac{P_i}{P} \right)^{\frac{1}{\gamma_u}}$$

For a constant volume vessel a differential form of the energy conservation equation is given as:

$$m \frac{de}{dt} - \frac{dQ}{dt} = 0 \quad (30)$$

The conservations of volume and internal energy are given by:

$$v = \frac{V}{M} = xv_b(P, T_b) + (1-x)v_u(P, S_{u,0})$$

$$e = \frac{E}{M} = xe_b(P, T_b) + (1-x)e_u(P, S_{u,0})$$

These differential equations are extended to the multiple burned gas zones for the multizone analysis;

$$\begin{aligned} \frac{dP}{dt} &= \frac{B}{C+D} \\ \frac{dT_U}{dt} &= \frac{v_u}{C_{pu}} \frac{\partial \ln v_u}{\partial \ln T} \left( \frac{B}{C+D} \right) \\ \frac{dT_b}{dt} &= -(1-x) \frac{v_u}{T_u} \frac{\partial \ln v_u}{\partial \ln T_u} \frac{T_b}{xv_b} \frac{\partial \ln T_b}{\partial \ln v_b} \cdot \frac{v_u}{C_{pu}} \frac{\partial \ln v_u}{\partial \ln T_u} \frac{\partial \ln v_u}{\partial \ln T_u} \left( \frac{B}{C+D} \right) - \end{aligned} \quad (31)$$

$$-\frac{T_b}{xv_b} \frac{\partial \ln T_b}{\partial \ln v_b} \left( x \frac{v_b}{P} \frac{\partial \ln v_b}{\partial \ln P} + (1-x) \frac{v_u}{P} \frac{\partial \ln v_b}{\partial \ln P} \right) \left( \frac{B}{C+D} \right) - \frac{T_b}{xv_b} \frac{\partial \ln T_b}{\partial \ln v_b} (v_b - v_u) \frac{dx}{dt}$$

Where:

$$B = \left( (v_b - v_u) + \frac{v_b}{C_{p,b}T_b} (h_b - h_u) \right) \frac{dx}{dt}$$

$$C = x \left( \frac{v_b^2}{C_{p,b}T_b} \left( \frac{\partial \ln v_b}{\partial \ln T_b} \right)^2 + \frac{v_b}{P} \frac{\partial \ln v_b}{\partial \ln P} \right)$$

$$D = (1-x) \frac{v_u^2}{C_{p,u}T_u} \left( \frac{\partial \ln v_u}{\partial \ln T_u} \right)^2 + \frac{v_u}{P} \frac{\partial \ln v_u}{\partial \ln P}$$

For the multizone analysis, the above equations are extended to N zones. Burned gas volume and radius are calculated from the following equations:

$$v_b = V - m_i(n-1) \left( \frac{R_u T_u}{P} \right)$$

and

$$r_b = R \left( V - m_i(n-1) \left( \frac{R_u T_u}{P} \right) \right)$$

The burning velocity by using multizone modal is:

$$S_u = \left( \frac{dp}{dt} \right) \left( \frac{dr_i}{dp} \right) \left( \frac{r_i}{r_b} \right)^2 \left( \frac{P_I}{P} \right)^{\frac{1}{\gamma_u}}$$

Being

$$\left( \frac{dp}{dt} \right) \rightarrow \text{Experimental data}$$

$$\left( \frac{dr_i}{dp} \right) \rightarrow \text{BOMB program}$$

## Conclusion

- A 10-zone model with 200 steps gives adequate accurate results
- A temperature difference exists between the first and the last burned gas-zones
- The relationship between the pressure rise and the mass fraction burned is nonlinear
- The burned gas temperature profile has an effect on the end pressure for methane
- The multizone burning velocity technique has been successfully used for the determination of the laminar burning velocities of methanol-air mixtures at varying equivalence ratios, temperatures and pressures
- Cellular flames have been found to exist in the test runs

## B. Mathematical Solutions for Explosions in Spherical Vessels

Equations, assumptions and previous solutions for central ignition of premixed gases in closed spherical vessels are reviewed. Three new categories of solution are presented:

1. -Approximate Computer Solution (Case 1)
2. -The Dimensionless Universal Expression (Case 2) -Does not require computer and has a good accuracy
3. -The Complete Computer Solution (Case 3) -The most accurate

## Introduction

A simple model is presented which is amenable to computer simulation and this is used to derive pressure-time curves in dimensionless form which are universally applicable for all explosions. From these curves, it is seen that corresponding dimensional curves are very sensitive to the value of burning velocity. Both temperature and pressure of the unburnt gas are changing during the explosion and data are required for the associated changes in burning velocity. With the availability of such data it has been worthwhile to develop a much more accurate computer model based upon finite difference techniques and less restrictive assumptions than formally used.

## The Basic Equations

- It is assumed that central ignition occurs in a rigid sphere and that a laminar flame that is smooth and spherical propagates outwards without any significant movement due to natural convection.
- The unburnt gas is isotropic
- Mass conservation gives:

$$m_o = m_u + m_b$$

$$\frac{dm_u}{dt} = -\frac{dm_b}{dt}$$

- The burnt gas fraction is:

$$n = \frac{m_b}{m_o}$$

- From the definition of burning velocity  $S_u$ :

$$\frac{dm_u}{dt} = -4\pi r_b^2 \rho_u S_u$$

Being  $r_b$  the radius of the inner boundary and  $\rho_u$  the density of unburnt gas.

- Volume conservation:

$$V_o = V_b + V_u$$

- The equation of state:

$$PV = mR_g T$$

$$\frac{d}{dt} [(R^3 - r_b^3) \rho_u] = 3r_b^2 \rho_u S_u$$

Where  $\rho_b$  is the mean density of the gas within the radius  $r_b$

## Simplified Analyses

- The unburnt gas is compressed isentropically:

$$(P\rho_u)^{\gamma_u} = \text{constant}$$

Fiock and Marvin result:

$$S_u = \frac{dr_b}{dt} - \frac{(R^3 - r_b^3)}{3r_b^2 \gamma_u P} \cdot \frac{dP}{dt}$$

- The fractional pressure rise is proportional to the fractional mass burnt

$$\frac{P - P_o}{P_e - P_o} = \frac{M_b}{M_o} = n$$

Being  $e$ : the condition when the explosion is completed.

### Case 1: The Approximate Computer Solution:

Pressure-time curves were obtained by increasing "n" elemental steps from 0 to 1. The computation procedure will be appreciated from the following equations:

$$\begin{aligned}
 P &= n(P_e - P_o) + P_o \\
 T_u &= T_o \left( \frac{P}{P_o} \right)^{\frac{\gamma_u - 1}{\gamma_u}} \\
 M_u &= M_o(1 - n) \\
 \frac{4}{3}\pi r_b^3 &= \frac{4}{3}\pi R^3 - \frac{m_U R_{gu} T_u}{P} \\
 \rho_u &= \frac{3m_u}{4\pi(R^3 - r_b^3)} \\
 dt &= -\frac{dm_u}{4_b^2 \rho_u S_u}
 \end{aligned}$$

### Case 2: The Dimensionless Universal Expression:

This attempts to obtain the maximum generality in the pressure time relationship.

$$\frac{dP}{dt} = \frac{3S_u \rho_u}{R \rho_o} (P_e - P_o) \left[ 1 - \left( \frac{P_o}{P} \right)^{\frac{1}{\gamma_u}} \frac{P_e - P}{P_e - P_o} \right]^{\frac{2}{3}}$$

Equation derived by Benson and Burgoyne. Dimensionless pressures and times are defined in terms of conditions at the end of the explosion:

$$\bar{P} = \frac{P}{P_e}; \bar{P}_o = \frac{P_o}{P_e}; \bar{t} = \frac{t}{t_e}$$

A mean flame speed,  $S_u$ , is defined by:

$$S_m = \frac{R}{t_e}$$

In nondimensional form the first equation becomes:

$$\frac{d\bar{P}}{d\bar{t}} = \frac{3S_u}{S_m} (1 - \bar{P}_o) \left( \frac{\bar{P}}{\bar{P}_o} \right)^{\frac{1}{\gamma_u}} \left[ 1 - \frac{1 - \bar{P}}{1 - \bar{P}_o} \left( \frac{\bar{P}_o}{\bar{P}} \right)^{\frac{1}{\gamma_u}} \right]^{\frac{2}{3}}$$

$$\frac{dP}{dt} = \frac{dn}{dt} (P_a - P_o)$$

$$\frac{dn}{dt} = \frac{3S_u}{r_b} \left[ n - 1 + \left( \frac{P}{P_o} \right)^{\frac{1}{\gamma_u}} \right]$$

Substituting:

$$S_s = S_u \left[ 1 + \frac{1}{\gamma_u \bar{P}} \left( \frac{R^3}{r_b^3} - 1 \right) \left( \bar{P} - 1 + (1 - \bar{P}_o) \left( \frac{\bar{P}}{\bar{P}_o} \right)^{\frac{1}{\gamma_u}} \right) \right]$$

Where  $S_s = \frac{dr_b}{dt}$

$$\left( \frac{r_b}{R} \right)^3 = 1 - \left( \frac{1 - \bar{P}}{1 - \bar{P}_o} \right) \left( \frac{\bar{P}_o}{\bar{P}} \right)^{\frac{1}{\gamma_u}}$$

$$\frac{dr_o}{dt} = S_s = S_u f(\bar{P})$$



$$\int_0^{t_e} dt = \int_0^R \frac{dr_b}{S_u f(\bar{P})}$$

If  $S_u$  is assumed to be constant through the explosion:

$$\frac{t_e S_u}{R} = \frac{S_u}{S_m} = \int_0^1 \frac{d\left(\frac{r_b}{R}\right)}{f(\bar{P})}$$

The problem presented by the fact that  $S_u$  is not constant but varies during the compression process accompanying combustion might be circumvented by the selection of an appropriate mean value of  $S_u$  for the whole explosion.

### Other Approximate Solutions

The simplicity of the Case 1 and Case 2 solutions rests upon the assumed equality of the fractional pressure rise and the fractional mass burnt. An alternative route involves a knowledge of the changes in the mean density of the burnt gas,  $\rho_b$ . This is not easy because of the non uniformity of the burnt gas temperature the gas burnt first attains a temperature higher than that burnt later. An assumption of the global isentropic compression law  $(P\rho_b)^{-\gamma_b} = \text{constant}$ . The temperature of the burnt gas was assumed to be that at the center of the vessel. The equations of mass and volume conservation, the perfect gas equation of state, and an assumed equality of the burnt and unburnt gas constants give rise to:

$$\frac{dP}{dt} = \frac{3\gamma_u S_u r_b^2 P \left(\frac{\rho_u}{\rho_b} - 1\right)}{R^3 \left[1 + \left(\frac{r_b}{R}\right)^3 \left(\frac{\gamma_u}{\gamma_b} - 1\right)\right]}$$

and

$$S_s = \frac{\rho_u}{\rho_b} S_u - \frac{r_b}{3\gamma_b P} \frac{dP}{dt}$$

Solutions of these equations were obtained numerically and presented in graphical form with  $P$ ,  $T_u$ ,  $r_b$ ,  $S_s$  and  $n$  plotted against  $t$ .

- Assumption 1:  $\gamma_b = \gamma_u = \gamma$
- Assumption 2: isothermal compression with  $T_u = T_o$ ,  $\gamma_b = \gamma_u = 1$

The analysis later were modified to take turbulence into account by the introduction of a constant,  $\alpha$ , such that the turbulent burning velocity was  $\alpha$  times the laminar burning velocity.

### Influence of Temperature and Pressure Changes on Burning Velocity

All solutions indicate their sensitivity to the numerical value of burning velocity. It is therefore necessary to know with some accuracy not only the initial value of burning velocity, but also the changes in it that occur during an explosion, as a result of the compression of the unburnt gas. Perlee considered the burning velocity of stoichiometric methane-air and combined the pressure dependence with their own temperature dependence to give:

$$S_u = \left(\frac{T_u}{t_o}\right)^2 \left(32,9 - 6,78 \ln\left(\frac{p}{p_2}\right)\right) \text{ cmsec}^1$$

Better agreement with experiment;

$$S_U = \left(S_{uo} - \beta_1 \ln\left(\frac{p}{p_0}\right)\right) \left(\frac{T_u}{T_o}\right)^{\beta_2} \text{ cmsec}^{-1}$$

Where  $S_{uo}$  the burning velocity at the initial conditions,  $\beta_1$   $\beta_2$  where constants chosen to give the best agreement with experiment. Noggy used:

$$S_u = S_{uo} \left( \frac{T_u}{T_o} \right)^2 \left( \frac{P_o}{P} \right)^\beta$$

For a variety of mixtures, in which  $\beta$  was zero for the isothermal and 0.25 for the adiabatic model.  $S_{uo}$  was chosen to give good agreement with experiment. Babkin and Kazachanko have carried out the most comprehensive experimental investigation of the influence of temperature and pressure during the period of constant pressure methane-air burning in a bomb explosion.

$$S_u = \frac{\rho_b}{\rho_u} S_s$$

It was assumed that the maximum temperature of the burnt gas was the ideal temperature.

### Accurate Analysis

In recent years computer based analysis have been developed with emphasis on chemical kinetic effects relevant to exhaust emissions. The present mark is less concerned with kinetics and more concerned with deriving accurate pressure-time solutions.

### Case 3: The Complete Computer Solution

Flame propagation is seen as the consumption of unburnt gas in small mass decrements  $dm_u$ . This mass does not become burnt gas instantaneously, but first passes through a reaction zone of finite thickness. The basic statement is that of conservation of total volume, which is made up the three volumes of unburnt, reacting and burnt gas. Consider the consumption of the nth elemental unburnt mass decrement,  $dm_n$ . This moves into the reaction zone with a temperature  $T_{u,n-1}$ , burns at the constant pressure  $P_{n-1}$ , and a proportion of the gas attains the ideal equilibrium temperature  $T_{f,n}$  for these conditions. This reaction must increase the pressure and in the model this is assumed to follow the constant pressure combustion and to be isentropic. The pressure throughout the vessel becomes  $P_n$  and the uniform unburnt gas temperature becomes  $T_{u,n}$ . At this stage the radius of the inner boundary of the unburnt gas is  $r_{b,n}$ ;

$$m_{u,n} = M_o - \sum_{i=1}^{i=n} dm_{u,i}$$

and

$$V_{u,n} = \frac{m_{u,n} R_{gu} T_{u,n}}{P_n}$$

Knowing that  $R_{g,u} = \text{constant}$ . The flame thickness,  $S_n$  between the temperatures  $T_{u,n-1}$  and  $T_{f,n}$ , can be calculated and the volume,  $V_{f,n}$ , associated with this flame thickness is found from;

$$V_{f,n} = \frac{4\pi}{3} [r_{b,n}^3 - (r_{b,n} - \rho_n)^3]$$

where

$$r_{b,n} = \left( R^3 - \frac{3}{4\pi} V_{u,n} \right)^{\frac{1}{3}}$$

The gas must be within the flame thickness before it is burnt,  $dm_{b,n}$ ;

$$dm_{b,n} = dm_{u,n} - (m_{f,n} - m_{f,n-1})$$

where  $m_{f,n}$  and  $m_{f,n-1}$  are masses within the flame thickness. The isentropic compression immediately following constant pressure combustion raises the freshly gas from a temperature  $T_{f,n}$  to  $T_{b,n}$ . Thus the volume of burnt gas produced during the decremental charge is:

$$V_{b,n} = \frac{[dm_{u,n} - (m_{f,n} - m_{f,n-1})] R_{gb,n} T_{b,n}}{P_n}$$

The total volume of burnt gas up to the nth decrement is;

$$V \frac{1}{P_n} \sum_{i=1}^{i=n} [dm_{u,i} - (m_{f,i} - m_{f,i-1})] R_{gbi,n} T_{bi,n}$$

$$M_{f,o} = 0$$

Volume conservation gives:

$$V_o = V_{u,n} + V_{f,n} + V_{b,n}$$

$$dt = \frac{-dm}{4\pi r_b^2 \rho_u S_u}$$

Equilibrium temperatures were computed from the JANAF. The presence of eleven chemical species was assumed in the methane-air explosions investigated, namely, CO, CO<sub>2</sub>, H<sub>2</sub>, H<sub>2</sub>O, OH, N<sub>2</sub>, N, NO, O, O<sub>2</sub> and from their concentrations could be obtained the burnt gas constant, R<sub>gb</sub>. Equilibrium constants were evaluated from values of Gibbs function. Enthalpies and entropies for each species were conveniently obtained from sets of polynomials derived from the JANAF data.

$$h_j^\circ = A_j T^4 + B_j T^3 + C_j T^2 + d_j T + E_j$$

and

$$s_j = A_j T^3 + B_j T^2 + C_j T + D_j \ln T F_j$$

$h_j^\circ$  and  $s_j^\circ$  : specific values

## Conclusions

- The basic equations and associated assumptions for flame propagation in spherical vessel have been reviewed.
- The fractional pressure rise is proportional to the fractional mass burnt
- The simplest solution to apply is that of Dimensionless Universal Expression
- The Complete Computer Solution is good agreement with accurate experimental values of the pressure time relationships.

## C. Equations for the Determination of Burning Velocity In A Spherical Constant Volume Vessel

### Introduction

Since burning velocities can not be measured directly, equations for calculating this property must be derived. It would appear that the various equations proposed have never been satisfactorily compared, either theoretically or by applying them to the results of a particular set of experiments.

### Derivation of Burning Velocity Equations

From the continuity equation

$$\frac{dm_u}{dt} = A \rho_u S_u$$

$S_u$  the normal velocity with which the unburnt gas crosses normal perpendicular to the flame front  
Combustion in a constant volume spherical vessel the mass of unburnt gas at any instant;

$$m_u = \frac{4}{3}\pi \left[ (R^3 - r_b^3) \frac{d\rho_u}{dt} - 3r_b\rho_u \frac{dr_b}{dt} \right]$$

$R$ : radius of the spherical vessel  $r_b$ : radius of the burnt gas Using these equations we find:

$$\frac{dm_u}{dt} = \frac{4}{3}\pi \left[ (R^3 - r_b^3) \frac{d\rho_u}{dt} - 3r_b^2\rho_u \frac{dr_b}{dt} \right]$$

$$S_u = \frac{dr_b}{dt} = \frac{(R^3 - R_o^3) d\rho_u}{3r_b\rho_u dt} = S_s - S_g$$

Considering adiabatic compression;

$$P = Cp_u^{\gamma_u}$$

Then we obtain the unburnt gas equation for the burning velocity of Fiock and Marvin

$$\frac{d\rho_u}{dt} = \frac{d\rho_u}{dP} \frac{dP}{dt} = \frac{\rho_u}{\gamma_u P} \frac{dP}{dt}$$

Substituting

$$S_u = \frac{dr_b}{dt} - \frac{(R^3 - R_B^3) dP}{3R_b^2\gamma_u P dt}$$

Alternative forms of these equations can be obtained by considering the burnt gas behind the flame front. Combustion in a constant volume vessel:

$$m_u = m_o - m_b$$

Thus:

$$\frac{dm_u}{dt} = - \frac{dm_b}{dt}$$

Then we are able to obtain:

$$S_b = \frac{1}{A\rho_u} \frac{dm_b}{dt}$$

$S_b$  property of the burnt gas. For a spherical flame font;

$$m_b = \frac{4}{3}\pi r_b^3 \bar{\rho}_b$$

The mean density,  $\bar{\rho}_b$ , allows us to obtain non-uniform properties of the gas behind the flame front due to recompression:

$$r_b \bar{\rho}_b = \frac{3}{r_b^3} \int_0^{r_b} \rho_b r^2 dr$$

when  $r_b = R$ ,  $\rho_b = \rho_o$ . In this equation total volume and mass are constant. From

$$\frac{dm_b}{dt} = \frac{4}{3}\pi \left[ r_b^3 \frac{d\bar{\rho}_b}{dt} + 3r_b^2 \bar{\rho}_b \frac{dr_b}{dt} \right]$$

Then we obtain:

$$S_b = \frac{\rho_b}{\rho_u} \frac{dr_b}{dt} + \frac{r_b}{3\rho_u} \frac{d\bar{\rho}_b}{dt}$$

Considering adiabatic compression:

$$P = C' \bar{\rho}_b^{\gamma_b}$$

Then:

$$\frac{d\bar{\rho}_b}{dt} = \frac{\bar{\rho}_b}{\gamma_b P} \frac{dP}{dt}$$

Finally we obtain the burnt gas equation for the burning velocity

$$S_b = \frac{\bar{\rho}_b}{\rho_u} \left[ \frac{dr_b}{dt} + \frac{r_b}{3\gamma_b P} \frac{dP}{dt} \right]$$

It is necessary to find the mean density of the burnt gas ( $\rho_b$ ). It is possible to avoid some difficulties.

$$\rho_b = \alpha \rho_o$$

Then:

$$\frac{d\bar{\rho}_b}{dt} = \rho_o \frac{d\alpha}{dt} = \rho_o \frac{d\alpha}{dP} \frac{dP}{dt}$$

The boundary conditions:

$$[\bar{\rho}_b]_{r_o=R} = r \bar{h} o_e = \rho_o$$

$$[\alpha]_{r_b=R} = \alpha_e = 1$$

From these formulas and the perfect gas equation we obtain:

$$\alpha = \frac{\bar{\rho}_b}{\rho_o} = \frac{\bar{m}_b}{m_o} \frac{T_o}{\bar{T}_b} \frac{P}{P}$$

$$\rho_o = \frac{\bar{m}_e P_e}{R \bar{T}_e}$$

$$\alpha = \frac{\bar{m}_b}{m_e} \frac{\bar{T}_e}{T_b} \frac{P}{P_e}$$

From this equations,  $\alpha$  is practically proportional to  $P$ ,  $\frac{d\alpha}{dP} = \frac{1}{P}$ . Even if the absolute values of  $\bar{m}_b$ ,  $\bar{T}_b$  and  $P$  are in error. Second equation must yield the contact value of  $\alpha$  (unity). The magnitude of any such errors can be estimated by evaluating  $\alpha$  at the end of the process from the first equation. The use of the second equation is preferred since errors in the determination of  $\bar{m}_b$ ,  $\bar{T}_b$  and  $P$  tend to be cancelled out. In fact, it becomes unnecessary to calculate mean values of the burnt gas temperature and molecular weight. For constant pressure combustion  $\frac{dP}{dt}$  is zero. Thus:

$$S_b = \frac{\rho_b}{\rho_o} \frac{dr_b}{dt} = \alpha_o S_g = \frac{S_g}{E_o}$$

Being  $E_o$  the initial expansion ratio. Lewis and Von Elbe:

$$n = \frac{m_o}{m_b}$$

$$\frac{dn}{dt} = \frac{1}{m_o} \frac{dm_b}{dt} = -\frac{1}{m_o} \frac{dm_u}{dt}$$

Substituting to:

$$\frac{dm_u}{dt} = -A \rho_u S_u$$

$$S_b = \frac{m_o}{A \rho_u} \frac{dn}{dt} = \frac{1}{3} \frac{R^3}{r_b^2} \frac{\rho_o}{\rho_u} \frac{dn}{dt}$$

During the early stages of combustion:

$$n = \frac{P - P_o}{P'_e - P_o}$$

Hence:

$$\frac{dn}{dt} = \frac{1}{P'_e - P_o} \frac{dP}{dt}$$

Eliminating  $r_b$ :

$$\frac{m_u}{m_o} = 1 - n = \frac{(R^3 - r_b^3)}{R^3 \rho_o} \rho_u$$

$$r_b = R \left[ 1 - (1 - n) \frac{\rho_o}{\rho_u} \right]^{\frac{1}{3}}$$

Then we obtain n's exact value:

$$n = \frac{r_b^3 \bar{P}_b}{R^3 \rho_o} = \alpha \frac{r_b^3}{R^3}$$

$$\alpha = \frac{\bar{m}_b \bar{T}_e P}{m_e \bar{T}_b P_e};$$

$$n = \frac{r_b^3 P}{R^3 P_e} = \frac{P \left( \frac{\rho_o}{\rho_u} \right) P}{P_e - \left( \frac{\rho_o}{\rho_u} \right) P}$$

Substituting.

$$r_b = R \left[ \frac{\frac{\rho_u}{\rho_o} - 1}{\frac{\rho_u}{\rho_o} - \alpha} \right]^{\frac{1}{3}}$$

## Introduction

Several equations have been used to calculate the burning velocities of a stoichiometric acetylene-air mixture, fired in a spherical vessel. Due to the low rate of pressure rise during the early stages of combustion two pressure traces were recorded.

- The Fiock and Marvin equation is the only one which doesn't require a knowledge of the properties of the burn gas. It has the disadvantage of magnifying small errors in the observations
- The Lewis and Von Elbe equation claimed to be accurate only over the initial stages

The calculated values of  $r_b$  are nearly always less than the observed radius. This difference suggests the existence of a reaction zone of significant thickness, particularly during the early stages when the spatial velocity is high. Values based on the low range pressure record are constantly nearer the observed radius than values from the high range record.

## Justification for Use of Proposed Burning Velocity Equation

The discrepancy between the calculated and observed flame radius suggests a lack of equilibrium in the burnt gas, probably confined to a reaction zone adjacent to the flame front. With the equations derived, an estimate of the degree of lack of equilibrium is possible. Consider the parameter  $\alpha$  which is defined as the ratio of the mean density of the burnt gas to the density of the unburnt mixture before ignition:

$$\alpha = \frac{\bar{\rho}_b}{\rho_o} = \frac{\bar{b}}{m_u \bar{T}_b} P P_o$$

Using the observed maximum pressure,  $P_e$ ,  $m_e$  and  $T_e$ , corresponding to final conditions in the burnt gas at the flame front, may be calculated assuming equilibrium conditions. An approximate value of  $\alpha$  may be calculated:

$$\alpha_e = \frac{m_e T_o P_e}{m_o T_e P_o}$$

In all cases  $\alpha_e$  is less than unity. Since the total mass of gas in the vessel remains constant, the mean density of the products when the flame has reached the bomb wall must equal the initial density of the unburnt mixture,  $\rho_b = \rho_o$ ; hence  $\alpha_e$  should have a value of unity at the end of the process. The discrepancy must therefore be attributed to  $P_e$  and  $\frac{m_e}{T_e}$  being too low.

- Consider  $P_e$ : an error could arise from
  - (a) Incorrect calibration of the pressure measuring system
  - (b) Inadequate transient response of the pressure transducer
 Use of the correct value would lower  $\alpha_e$  still further.

Consider  $\frac{m_e}{T_e}$  instead of  $\frac{\bar{m}_e \bar{c}_e}{T_e}$

- (a) The temperature at the flame front is less than that at the centre of the vessel. Thus  $T_e$  is less than  $\bar{T}_e$ .
  - (b) The difference between  $m_e$  and  $\bar{m}_e$  is small compared with the difference between  $T_e$  than  $\bar{T}_e$ .
- Hence the use of mean temperatures to calculate  $\alpha_e$  would yield even lower values than those obtained by using flame front temperatures.

The only term left to account for the discrepancy between the deserved and expected values of  $\alpha_e$  is the temperature of the burnt gas. It appears that the calculated equilibrium value of flame front temperature is too high. There are two factors which may account for the calculated value of  $T_b$  being too high:

- (a) Combustion may not occur adiabatically due to heat loss. But, the quantity of heat loss by radiation up to the time the flame reaches the bomb wall is negligible. Conductive heat loss, due to buoyancy, is likely to be longer for slow burning mixtures, and should lead to lower values of  $\alpha_e$  for the rich and lean mixtures tested. Therefore, heat loss can not explain discrepancy.
- (b) The assumption that equilibrium is attained immediately behind the flame front may not be justified: insufficient time may be available for the reactions to go to completion. If this is so then at any air/fuel ratio the thickness of such a reaction zone should increase with flame speed.

The lowest value of  $\alpha_e$  coincides with the greatest observed spatial velocity. Thus if a non-equilibrium condition exists at the end of the process ( $\alpha_e < 1$ ), on even greater departure from equilibrium probably exists over the initial stages since the spatial velocity is then higher. Using the alternative approximate expression for  $\alpha$ :

$$\alpha = \frac{m_b T_e P}{m_e T_b P_e}$$

which must yield the correct value of  $\alpha_e$  (unity). All previous burning velocity equations have been based on the assumption that chemical equilibrium exists in the burnt gas. In the burning velocity equation any such lack of equilibrium is partly allowed for by using the dimensionless density ratio  $\alpha$  calculated from the above equation.

## D. Burning Velocity Measurement of Fluorinated Compounds By The Spherical-Vessel Method

### Abstract

Burning velocity has been measured using the spherical vessel (SV) method for four hydrofluorocarbons (HDCs). Experiments were conducted for initial pressures in the range 78-108 kPa and initial temperatures in the range 280-330 K, over wide ranges of HCF-air. The burning velocities were determined from the rate of pressure increase by applying a spherical-flame propagation model. It is found that the SV method is adequate for determining the burning velocity for weakly flammable HCFs as well as for moderately flammable compounds. The magnitude of the burning velocity is strongly dependent on the ratio of H atoms to F atoms in the HFC molecules.

## Introduction

There are a number of flammable compounds among the alternatives. In order to ensure safe use of these substances, assessment of their flammability is important. For the burning velocity measurement, numerous techniques have been developed. The method of measurement is in general chosen according to the properties of compounds and experimental requirements. Fluorinated compounds usually have low burning velocities. In addition, some refrigerants and cleaning solvents have a higher boiling point than room temperature. The SV method is more appropriated than the Bunsen method. It has been widely used for flammable gases such as hydrogen and hydrocarbons because it provides experimental accuracy as well as operational simplicity: the burning velocity of a compound together with its temperature and pressure dependence is obtained simultaneously by measuring the pressure time history in the vessel. There is a concern about using the SV method for weakly flammable compounds. It is necessary to assume that the flame front is spherical and smooth. But for a compound with low burning velocity such as  $NH_3$ , the buoyancy force may distort the flame front which can not be regarded as spherical.

## Result and Discussion

### **Method of Analysis The Data Obtained With The SV Method**

The burning velocity  $S_u$ :

$$S_u = \frac{R}{3} \left[ 1 - (1-x) \left( \frac{P_o}{P} \right)^{\frac{1}{\gamma_u}} \right]^{-\frac{2}{3}} \left( \frac{P_o}{P} \right)^{\frac{1}{\gamma_u}} \frac{dx}{dt}$$

In order to use this equation, we have to obtain the relationship of P with x,  $\gamma_u$ ,  $r_f$ , and burned and unburned gas temperatures  $T_u$  and  $T_b$ . The obtained  $S_u$  has been fitted to the following:

$$S_u = S_{uo} \left( \frac{T}{T_s} \right)^\alpha \left( \frac{P}{P_s} \right)^\beta$$

Taking into account that:  $T_s = 298K$

$P_s = 1atm$

$S_{uo}$  = burning velocity at  $T_s, P_s$

$\alpha$  and  $\beta$ : coefficients of temperature and pressure dependence.

$S_{uo}, \alpha$  and  $\beta$  are dependent on  $\phi$ ;  $S_{uo} = S_{uo,max} + S_1(\phi - \phi_{max})^2 + S_2(\phi - \phi_{max}^3)\alpha = a_1 + a_2(\phi - 1)\beta = b_1 + b_2(\phi - 1)$

## Conclusion

The present study focus on determination of burning velocities of HFCs. The burning velocities of HFC-32, HFC-143, HFC-143a and HFC-152a together with  $CH_4$  and  $C_3H_8$  were investigated.

Burning velocities were determined by analyzing the pressure time profiles in the spherical vessel and were checked by direct observation of flame propagation using the schlieren photograph in a wide range of concentrations.

Direct measurement of flame propagation showed that a flame with a longer burning velocity is less affected by buoyancy than those with smaller burning velocity.

For HFC-32 and HFC-143a concentrations that are far from stoichiometric, the flame shapes were distorted by buoyancy. For the concentrations that were used for the measurement, the burning velocity was obtained with good accuracy and buoyancy affects were negligible. Thus the SV method is appropriate for determining the burning velocity even for weakly flammable HFCs.



# E. Impact of Dissociation and End Pressure on Determination of Laminar Burning Velocities In Constant Volume Combustion

## Abstract

Determining laminar burning velocities  $S_u$  from the pressure trace in constant volume combustion requires knowledge of the burnt fraction as a function of pressure  $x(p)$ .  $x(p)$  is either determined via numerical modeling or via the oversimplified assumption that  $x(p)$  is equal to the fractional pressure rise.

In this paper we systematically compare our analytical models with a numerical two-zone model and with a 1D unsteady simulation (1DUS) of a spherical stoichiometric methane-air flame in a constant volume.

Results indicate that our analytical models reasonable describe the burnt fraction as a function of fractional pressure rise. However the  $x(p)$  relation also involves the end pressure  $p_e$ . Its value significantly affects  $S_L$  and influenced by dissociation.

Evaluating  $p_e$  from an equilibrium code, in combination with the analytical  $x(p)$  model, provides  $S_L$  is achieved using numerical  $x(p)$  models that account for dissociation also for intermediate stages.

## Introduction

Laminar burning velocities of a combustible mixture can be obtained by recording the pressure  $p$  as a function of time in a constant volume vessel.

The burning velocity values ( $S_u$ ) are obtained for a range of pressures and temperatures in one single experiment. Only the pressure is needed to determine  $S_L$

In the analysis of pressure data, a set of assumptions commonly made, including uniformity of pressure, negligible external heat loss or gain (ignition), no buoyancy effects, isentropic compression of the burnt gas, and an infinitely thin and spherical flame front with no heat transfer between the burnt and unburnt zones. Using these assumptions,  $S_u$  can be related to the pressure trace through a differential equation:

$$\frac{dp}{dt} = \frac{3}{R} \left( \frac{dx}{dp} \right)^{-1} \left[ 1 - \left( \frac{P_i}{P} \right)^{\frac{1}{\gamma_u}} (1-x) \right]^{\frac{2}{3}} \left( \frac{P}{P_i} \right)^{\frac{1}{\gamma_u}} S_L$$

Being:

$P_i$ : initial pressure

$\gamma_u$ : isentropic exponent of the unburnt gas

R: vessel radius

x: burnt mass fraction

Relation between x and p must be known

Lewis and von Elbe argue that relation between x and p is very close to linear, and they introduce the relation:

$$x = \frac{p - p_i}{p_e - p_i}$$

In the derivation of analytical relations, we have to assume perfect gas behaviour of both unburnt and burnt gas. This implies (besides having constant specific heats) that the average molar mass before and after combustion remains constant. Hence, shifting chemical equilibrium due to the changing temperature of successively burnt shells is not taken into account.

A second point of concern is that analytical  $x(p)$  relations require the end pressure  $p_e$  as input. The  $P_e$  value required in the evaluation is necessarily the theoretical end pressure (which would be achieved when a perfectly spherical and adiabatic flame would develop in a spherical vessel in the absence of gravity).

Finally, we will show how the combined effect of  $x(p)$  model and end pressure affects the differences between  $S_u$  values.

Stoichiometric methane-air will be used.

## Theory

Analytical models for both two and multiple zones are briefly described. The most restrictive simplification is the assumption of perfect gas behaviour.

The two-zone analytical model neglects the burnt temperature gradient. This simplification was slow not to affect the  $x(p)$  results within a perfect gas. However, when both a burnt temperature gradient and dissociation are allowed, this may no longer hold true: enhanced dissociation near the core of the vessel may affect the mass-averaged burnt temperature leading to different results for  $x(p)$  as wall.

### Analytical Two-Zone Model

In a two zone model, both the burnt and unburnt zones have uniform temperatures and compositions: Conservation of specific volume:

$$v_t = xv_b + (1 + x)v_u$$

Conservation of specific internal energy:

$$e_t = xe_b + (1 + x)e_u$$

The specific internal energy is evaluated: Unburnt mixture

$$e_u = C_{vu}(T_u - T_o) + D_e$$

Burnt mixture

$$e_b = C_{vb}(T_b - T_o) + D_e$$

Being  $T_o$ : the reference temperature. The above equations can be manipulated to:

$$x = \frac{p - p_i f(p)}{p_e - p_i f(p)}$$

Where:

$$f(p) = \frac{\gamma_b - 1}{\gamma_u - 1} + \left( \frac{\gamma_u - \gamma_b}{\gamma_u - 1} \right) \left( \frac{P}{P_i} \right)^{\frac{\gamma_u - 1}{\gamma_u}}$$

The resulting equation obeys energy conservation.

This equation does not hold true for linear relation between  $x$  and  $p$ . This observation can be attributed to an underestimation of entropy production by the linear model.

The end pressure  $p_e$  in the two-zone model is obtained from conservation of internal energy for  $x = 1$ :

$$cv_u(T_i - T_o) + D_e = cv_b(T_e - T_o)$$

The unburnt specific heat is evaluated at  $T_i = 298,15K$

Specific heat of the burnt gas evaluated at  $\frac{(T_i + T_e)}{2}$

In this way we have;

$$Cp_u = 1078 Jkg^{-1}K^{-1}$$

$$Cp_u = 777 Jkg^{-1}K^{-1}$$

$$Cp_b = 1425 Jkg^{-1}K^{-1}$$

$$Cv_b = 1124 Jkg^{-1}K^{-1}$$

and

$$\gamma_u = 1,39$$

$$\gamma_b = 1,27$$

$$\Delta e = 276 \text{MJkg}^{-1}$$

$$T_e = 2744 \text{K}$$

$$P_e = 9,2 \text{bar}$$

### Analytical Multi-Zone Model

The approach sketched above for two zones can be extended to multiple neglecting heat loss to the vessel wall.

$$v_t = \sum_{j=1}^{n=1} x_j v_{bj} + x_n v_{bn} + \left[ 1 - \sum_{j=1}^1 x_j \right] v_u$$

$$e_t = \sum_{j=1}^{n=1} x_j e_{bj} + x_n e_{bn} + \left[ 1 - \sum_{j=1}^1 x_j \right] e_u$$

Shells with lower indices have burnt previously, and are compressed in a isentropic way during burning of the nth shell. For this reason, the nth terms are treated differently. Specific heats are taken identical as in the two-zone model. Heat exchange between zones are neglected. The total burnt fraction x after burning of N zones:

$$x = \sum_{n=1}^N x_n$$

### Numerical Two-Zone Model

The numerical two-zone model starts from the conservation equations. Heat losses are neglected. The perfect gas assumption is dropped. Temperature dependent caloric properties are evaluated from polynomial fits. The numerical model was run in two modes: **"No dissociation"**, complete combustion is assumed into  $CO_2$  and  $H_2O$ .

**"Equilibrium"**, the burnt gas is assumed to be in chemical equilibrium. Depending on pressure and temperature, the composition of the burnt mixture is computed using an equilibrium solver.

The conservation equations are solved for x and  $T_b$  for every incremental pressure step. The pressure profile is input by the user.

The model is run until the burnt mass fraction reaches unity, the corresponding pressure at that point is the end pressure  $p_e$ .

### Conclusions

Evaluation of laminar burning velocities  $S_u$  from the pressure trace in constant volume combustion necessarily requires the burnt mass fraction as a function of pressure.

Manipulation of volume and energy conservation laws for perfect gases leads to an analytical x(p) relation that is as easy to implement as the linear one. The derivation requires the assumption of perfect gas behaviour, thus neglecting dissociation and other potentially important effects.

The numerical models used for comparison allowed for temperature dependent specific heats and dissociation. Both effects were shown to affect  $x(p)$ , with about equal magnitudes.

The one-dimensional unsteady simulation was also used to confirm that flame stretch does not affect  $x(p)$  for stoichiometric combustion of methane with air.

We have demonstrated new relations for  $x$  and  $p$  that well capture deviation from the linear relation found from the numerical models. This proves that neglect of the difference between burnt and unburnt specific heat ratios is the major pitfall of the linear approximation.

Any analytical  $x(p)$  relation requires the end pressure as input. Its value affects  $S_L$  values is achieved using a numerical model that correctly accounts for dissociation throughout the experiment.